

# Kinetics of Conversion of Air Bubbles to Air-Hydrate Crystals in Antarctic Ice

P. B. Price

Physics Department, University of California, Berkeley, CA 94720

April 26, 2024

## Abstract

The depth-dependence of bubble concentration at pressures above the transition to the air hydrate phase and the optical scattering length due to bubbles in deep ice at the South Pole are modeled using diffusion-growth data from the laboratory, taking into account the dependence of age and temperature on depth in the ice. The model fits the available data on bubbles in cores from Vostok and Byrd and on scattering length in deep ice at the South Pole. It explains why bubbles and air hydrate crystals co-exist in deep ice over a range of depths as great as 800 m and predicts that at depths below  $\sim 1400$  m the AMANDA neutrino observatory at the South Pole will operate unimpaired by light scattering from bubbles.

Ancient air is known to be trapped in polar ice at depths below the layer of firn (i.e., porous) ice. Early investigations showed that the air was trapped in bubbles which decreased in size and concentration with increasing depth. To account for the disappearance of bubbles at great depth, Miller (1) predicted that the bubbles would convert into a clathrate hydrate phase at depths corresponding to a pressure greater than that for formation of that phase. He showed that the phase consists of a cubic crystal structure in which  $O_2$  and  $N_2$  molecules from air are trapped in clathrate cages. If  $O_2$  and  $N_2$  occur in atmospheric proportions, the crystals are usually referred to as air hydrate crystals. The hatched region in Fig. 1 shows Miller's calculated curves for the temperature-dependence of the formation pressure for nitrogen-hydrate and for air-hydrate, displayed on a scale in which pressure has been converted to depth in ice. The curves labeled for ice at four Antarctic sites and two Greenland sites give temperature as a function of depth (2-6). Koci (6) modeled the temperature vs depth at South Pole, using the known surface temperature of  $-55\text{ C}$  and fixing the temperature at bedrock at the pressure melting temperature. *In situ* measurements (7) by AMANDA at depths from 800 to 1000 m gave temperatures that agreed with Koci's model to within 0.3 C.

In Fig. 1, square points indicate the depths in cores below which air bubbles are not observed. The triangular points indicate the depths below which air hydrate crystals are observed. Over a wide range of depths between each triangle and square, both bubbles and air hydrate crystals are seen to co-exist. For Vostok and Byrd cores, quantitative measurements have been made of concentrations and sizes of bubbles (8,9) and air hydrate crystals (10,11). For Dome C, Dye-3, and Camp Century cores, Shoji and Langway (12,13) reported only qualitative data on air hydrates. For the South Pole, no deep core has yet been obtained.

This paper poses solutions to several puzzles: Why do bubbles and air hydrate crystals co-exist over a range of depths as great as 800 m? In particular, why does it take so long for bubbles to disappear at pressures at which they are unstable against the phase transition? Why do the depths of disappearance of bubbles in various cores not show some systematic dependence on depth or temperature? Based on the measurements on bubbles at Vostok and Byrd, can we predict the concentration of bubbles as a function of depth in ice at the South Pole? The last question is of great importance to the AMANDA project (14,15), which involves implanting long strings of large photomultiplier tubes at great depths in South Pole ice in order to detect Čerenkov light from muons produced in high-energy neutrino interactions. Only if the array is located in bubble-free ice can the direction of a muon be precisely determined by measuring the arrival times of the Čerenkov wavefront at each of the phototubes.

Several studies of the transformation of air bubbles into air hydrate crystals have been done in pressure cells on timescales up to a few days at temperatures from  $-20\text{ C}$  to  $-2\text{ C}$  and at pressures up to  $\sim 8\text{ MPa}$ . Using a high-pressure cell on a microscope stage, Uchida et al. (16) studied the growth of air hydrate crystals on the walls of bubbles in a sample of Vostok core taken from a depth of 1514 m. Because of relaxation after recovery of the core, the original air hydrate crystals had converted back into bubbles before Uchida et al. started the experiment. They observed the growth rate of air hydrate crystals as a function of supersaturation,  $\delta P/P_e$ , at temperatures just below the melting point of ice. Here  $P$  = hydrostatic pressure on the system and  $P_e$  = equilibrium pressure at the phase boundary. They found that for  $\delta P/P_e > 0.35$  the crystals grew as spherical shells coating the bubble walls.

Continuing this line of research, Uchida et al. (17) showed that two activation energies were involved. Before a thin shell of air hydrate crystal had completely coated the wall of a bubble, they found  $E_s = 0.52 \pm 0.17\text{ eV}$ . After it had fully coated the bubble wall, they found a higher value,  $E_s = 0.9 \pm 0.1\text{ eV}$ , for thickening of the shell. In the early growth stage, it seemed clear that the process occurred by diffusion of water molecules through the normal ice to uncoated sites on the bubble wall, because their activation energy was consistent with that for self-diffusion,  $0.57 \pm 0.1\text{ eV}$  (18). The higher value, for the later growth stage, applied to diffusion through the air hydrate itself. With the assumption (unjustified) of a linear radial growth rate, they concluded that air hydrate crystals would form far too quickly to account for the broad range of depths over which bubbles and air hydrate crystals co-exist in polar ice cores. They suggested that the rate-limiting

process is nucleation, not diffusion.

Ikeda et al. (19) subjected artificial ice to various hydrostatic pressures at 270 K and measured the fraction of bubbles converted to air hydrate crystals in 16 days. They assumed, without proof, that the rate-limiting step in the transformation is nucleation. After failing to account for the observed rates by homogeneous nucleation theory, they drew the unsatisfying conclusion that the mechanism must be heterogeneous nucleation, but with a different parameter for each data point! [See their Fig. 7.]

Examination of the various models of nucleation led us to the conclusion that none of them provides a satisfactory explanation for the data presented in Fig. 1. Homogeneous nucleation requires such an enormous supersaturation, defined as  $\delta P/P_e$ , that it almost never occurs in nature. Heterogeneous nucleation on a foreign surface at low supersaturation is far more likely. The presence of a bubble wall serves as a suitable nucleation site. Fletcher (20) calculated nucleation rates as functions of supersaturation, size of the substrate on which nucleation occurs, and surface energies of the substrate and the nucleated phase. For typical bubble sizes and reasonable values of surface energies, his results show that nucleation would be rapid at supersaturations below 0.2, whereas for the data in Fig. 1, bubbles are still present at values of  $\delta P/P_e$  as large as 2. Further, the presence of one or more screw dislocations in the ice ending at a bubble surface would reduce the needed supersaturation to a value less than 0.01 (21). Typical dislocation densities in even well- annealed crystals are high enough ( $> 10^4 \text{ cm}^{-2}$ ) to ensure their presence at bubble walls.

I assert that the rate-limiting step in the phase transition is diffusion rather than nucleation. To show this I carried out a diffusion calculation that takes into account the time and temperature as a function of depth for the Vostok and Byrd sites. I converted depth to time for each core using age vs depth data in (7). I assumed that there is no nucleation barrier and that the long time-scale for the disappearance of bubbles is due to slow diffusion. I assumed two diffusion steps. The first step consists of diffusion of water molecules through ice to a bubble wall, in which  $D(T)$  is taken to be  $D_0 \exp(-E_s/kT)$ , with  $E_s = 0.57 \text{ eV}$  and  $D_0 = 1.2 \text{ cm}^2 \text{ s}^{-1}$  as measured (18) for self-diffusion in ice (22).

The second step consists of diffusion of water molecules through a spherical shell of air hydrate coating the bubble wall and growing in thickness. For the activation energy for diffusion in air hydrate I adopted the value  $E_s = 0.9 \pm 0.1 \text{ eV}$  measured for the growth of the air hydrate layer (17). [The authors in ref. 17 did not measure  $D_0$ .] After reaching the inner radius of the hollow air hydrate shell, water combines with air molecules and causes the crystal to thicken, with negligible activation barrier (23). At  $P \sim 10^2 \text{ atm}$ ,  $T \sim 230 \text{ K}$ , the concentration of air in the bubble,  $\sim 4 \times 10^{21} \text{ cm}^{-3}$ , is comparable to that in an air hydrate crystal with the same volume (8 cages per unit cell;  $\sim 80\%$  occupancy; cubic structure; cube edge = 1.7 nm). Thus, the supply of air is adequate for full conversion from (air + ice) to the hydrate phase.

The first step, of water molecules diffusing in ice to the bubble wall, occurs so rapidly that one can apply the boundary condition that  $C(r > a) = C_0$  for all time, where  $a$  is the bubble radius and  $C_0$  is the initial concentration of interstitial  $\text{H}_2\text{O}$  molecules everywhere outside the bubble. The problem is that of spherically symmetric diffusion with  $C = 0$  at  $t = 0$  inside the bubble and  $C = C_0$  at the wall (24). The justification for taking  $C = 0$  at  $t = 0$  inside the bubble is that all of the water vapor inside the bubble ( $\sim 10^{15}$  molecules  $\text{cm}^{-3}$  at -40 C) is exhausted in creating an infinitesimally thin shell of air hydrate, after which further water must diffuse through the air hydrate shell (25).

As a function of time, the amount of mass transported through the bubble wall due to diffusion grows, as given by eq. 6.21 of (24) (with the running index  $n$  replaced by  $j$  to avoid ambiguity with my symbol for bubble concentration)

$$\frac{M(t)}{M(\infty)} = 1 - \frac{6}{\pi^2} \sum_{j=1}^{\infty} \frac{1}{j^2} \exp(-j^2 \pi^2 D(T)t/a^2) \quad (1)$$

where  $a$  = bubble radius. Equating this to the probability of disappearance per bubble yields for the fractional concentration remaining after time  $t$

$$\frac{n(t)}{n_0} = \frac{6}{\pi^2} [\exp(-\pi^2 I(t)/a^2) + \frac{1}{4} \exp(-4\pi^2 I(t)/a^2) + \dots] \quad (2)$$

$$\text{with } I(t) = \int_{t_e}^t D_0 \exp(-E_s/kT) dt' \quad (3)$$

The integral  $I(t)$  takes into account the fact that  $D(T)$  and  $t$  change with depth. Its lower limit corresponds to the age of the ice at the transition pressure. The second term in eq. 2 contributes only at short times, and higher order terms can be neglected.

I fitted eq. 2 to the extensive Vostok data (8) on bubble concentrations at depths greater than 500 m, the depth corresponding to the transition pressure, at which air hydrate crystals are first observed. With  $D_0$  as a fitting parameter, I found that  $D_0 = 2100 \text{ cm}^2 \text{ s}^{-1}$  gave acceptable fits to both the Vostok data and the Byrd data (9) on bubble concentration as a function of depth.

Figure 2 displays values of  $1/\lambda_{bub} \equiv n\pi r^2$ , the reciprocal of the bubble-to-bubble scattering length, as a function of depth,  $z$ , for Vostok, Byrd, and South Pole. The experimental points use data on bubble concentration,  $n(z)$ , and radius,  $r(z)$ , for Vostok and for Byrd. The data for South Pole are from *in situ* light scattering at depths of 800 to 1000 m (15). The curves show the results of applying the diffusion model to the three sets of data.  $n(t)$  is calculated from eq. 2, taking  $a = a_0$ , the mean radius at the dissociation pressure. The observed values are  $a_0 = 68 \mu\text{m}$  for Vostok and  $130 \mu\text{m}$  for Byrd. In the absence of data on  $a_0$  for the South Pole, I assumed the same value as for Vostok, since those two sites have similar elevations, surface temperatures, atmospheric pressures, and hydrate dissociation pressures (see Fig. 1), which are rather different from those at Byrd. To compute the curve for  $1/\lambda_{bub}$ , I assumed that  $r = a_0(P_e/P)^{\frac{1}{3}}$  due to hydrostatic pressure. The fits to the data for Vostok and Byrd are quite good and lend confidence to the predicted dependence of  $1/\lambda_{bub}$  on depth for the South Pole (26).

The diffusion-growth model provides a solution to the puzzles listed in the introduction. The reason that bubbles do not all convert into air hydrate crystals at the phase transition pressure, and the reason for the great range of depths at which both air hydrate crystals and bubbles co-exist, is that the time required for water molecules to diffuse through a growing shell of air hydrate at ambient ice temperature is extremely long. The diffusion coefficient for water in air hydrate,  $D(T) = D_0 \exp(-E_s/kT)$ , with  $D_0 = 2100 \text{ cm}^2 \text{ s}^{-1}$ , is orders of magnitude smaller than for self-diffusion in hexagonal ice. For example, at -46 C, the temperature of South Pole ice at a depth of 1 km,  $D = 2.2 \times 10^{-17} \text{ cm}^2 \text{ s}^{-1}$  for water in air hydrate, whereas  $D = 2.65 \times 10^{-13} \text{ cm}^2 \text{ s}^{-1}$  for water in hexagonal ice. The reason for the apparent lack of organization of the data on bubble disappearance in Fig. 1 is that the depth is the wrong variable to use. Due to large variations in snow accumulation rate from one polar site to another, depth is not universally related to time. Only when data are plotted on a graph of time vs reciprocal of temperature does the correlation become clear. When applied to laboratory data on rate of decrease of concentration of bubbles in ice near the melting point (19), the model gives results consistent with the data.

The model predicts that in deep ice at the South Pole, the bubble-to-bubble scattering length is  $\sim 6$  m at 1300 m, 20 m at 1400 m, and 130 m at 1500 m. For an AMANDA phototube spacing of 20 m, bubbles will cease to degrade imaging at depths greater than  $\sim 1400$  m.

This work was supported in part by National Science Foundation grant PHY-9307420.

## REFERENCES

1. S.L. Miller, *Science* **165**, 489 (1969).
2. For Dome C, see C. Ritz, L. Lliboutry, C. Rado, *Ann. Glaciology* **3**, 284 (1982).
3. For Dye 3, see D. Dahl-Jensen and S. J. Johnsen, *Nature* **320**, 250 (1986).
4. For Byrd and Camp Century, see W. F. Budd and N. W. Young, in *The Climatic Record in Polar Ice Sheets*, G. de Q. Robin, Ed. (Cambridge Univ. Press, Cambridge, 1983), p. 150.
5. For Vostok, see C. Ritz, *Ann. Glaciology* **12**, 138 (1989).
6. A model for temperature vs depth at the South Pole was developed by Bruce Koci, unpublished material.
7. AMANDA Collaboration (P. Askebjerg *et al.*), submitted to *J. Glaciology* (1994).
8. N.I. Barkov and V.Ya. Lipenkov, *Mat. Glyatsiol. Issled.* **51**, 178 (1984).
9. A.J. Gow and T. Williamson, *J. Geophys. Res.* **80**, 5101 (1975).
10. V.Ya. Lipenkov, *Mat. Glyatsiol. Issled.* **65**, 58 (1989).
11. T. Uchida, T. Hondoh, S. Mae, V. Ya. Lipenkov, P. Duval, *J. Glaciology* **40**, 79 (1994).
12. H. Shoji and C.C. Langway, Jr., *Nature* **298**, 548 (1982).
13. H. Shoji and C.C. Langway, Jr., *J. Phys. (Paris)* **48**, colloq. C1, 551 (Supplement au 3) (1987).
14. S.W. Barwick *et al.*, *J. Phys. G (Nucl. Part. Phys.)* **18**, 225 (1992).
15. AMANDA Collaboration (P. Askebjerg *et al.*), submitted to *Science* (1994).
16. T. Uchida *et al.*, in *Proc. Inter. Conf. on Physics and Chemistry of Ice* (ed. N. Maeno and T. Hondoh), Hokkaido University Press, Sapporo, 1992, pp. 121-125.
17. T. Uchida *et al.*, in *Fifth Inter. Symp. On Antarctic Glaciology*, to be published (1994).
18. K. Goto, T. Hondoh, A. Higashi, *Jap. J. Appl. Phys.* **25**, 351 (1986).
19. T. Ikeda, T. Uchida, S. Mae, *Proc. NIPR Symp. Polar Meteorog. Glaciol.* **7**, 14 (1993).
20. N. H. Fletcher, *J. Chem. Phys.* **29**, 572 (1958).
21. W.K. Burton, N. Cabrera, F.C. Frank, *Phil. Trans. Roy. Soc. (London)* **A 243**, 299 (1951).
22. The authors of (18) showed that self-diffusion in ice occurs by diffusion of interstitial water molecules rather than vacancies.
23. An alternative possibility, that air molecules diffuse through the air hydrate shell and convert ice to air hydrate at the bubble boundary, is ruled out experimentally. Uchida *et al.* (16,17) observed that air hydrate crystals grow inwardly, causing bubbles to shrink in size and eventually disappear.
24. J. Crank, *The Mathematics of Diffusion* (Clarendon Press, Oxford, 1975).
25. This assumes that the vapor pressure of water at the surface of an air hydrate crystal is much smaller than at the surface of an ice crystal.

26. An alternative procedure is to fix  $D_0 = 1.2 \text{ cm}^2 \text{ s}^{-1}$ , the same for diffusion of water in air hydrate as in ice, and to treat  $E_s$  as a fitting parameter. Doing this leads to acceptable fits to the Vostok and Byrd data but with  $E_s = 0.75 \text{ eV}$ , which is outside the standard error claimed in (11). The resulting curves for  $1/\lambda_{bub}$  for Vostok, Byrd, and South Pole are similar to those calculated with  $D_0 = 2100 \text{ cm}^2 \text{ s}^{-1}$ ,  $E_s = 0.9 \text{ eV}$ . The conclusion is that the present data do not enable one to determine both  $D_0$  and  $E_s$  independent of laboratory data.

## FIGURE CAPTIONS

1. Temperatures as a function of depth in ice, compared with equilibrium pressures (converted to depths) for co-existence of the (bubble + ice) phase and the air hydrate phase. Upper boundary of the hatched region is for nitrogen-clathrate-hydrate; lower boundary is for air-clathrate-hydrate. Square points indicate the depths in cores below which air bubbles are not observed. The arrow on the square symbol for Dome C indicates that air hydrate crystals were present to the bottom of the core. Triangular points indicate the depths below which air hydrate crystals are observed.
2. Reciprocal of bubble-to-bubble scattering length,  $1/\lambda_{bub} = n\pi r^2$ , as function of depth. Data for Vostok (8) and Byrd (9) were obtained with microscopic examination of core samples in a cold laboratory; data for South Pole were obtained by *in situ* measurement of optical scattering (15). Upper solid triangles assume forward scattering from smooth-walled bubbles; lower solid triangles assume isotropic scattering from rough-walled bubbles. Hydrostatic pressure curve shows effect of shrinkage of bubble size without change of concentration. Calculated curves for the three sites show the effect of a decrease in bubble concentration as a function of time due to diffusion of H<sub>2</sub>O molecules through air hydrate crystal walls.

This figure "fig1-1.png" is available in "png" format from:

<http://arxiv.org/ps/astro-ph/9501073v2>



This figure "fig2-1.png" is available in "png" format from:

<http://arxiv.org/ps/astro-ph/9501073v2>

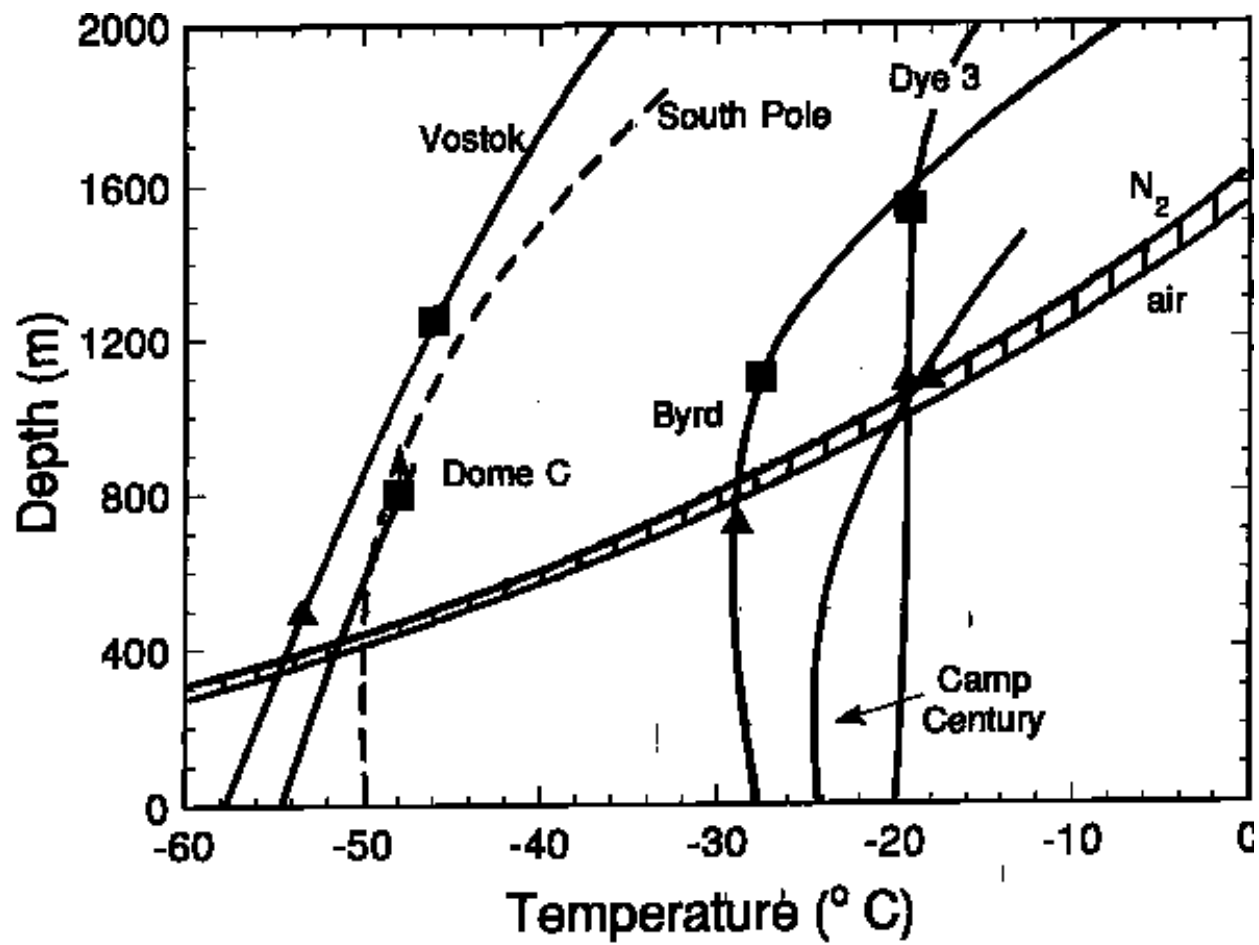


Figure 1

